ACS OMEGA

Article

Cite This: ACS Omega 2019, 4, 21900−21908

http://pubs.acs.org/journal/acsodf

Duplex Electrochemical DNA Sensor to Detect *Bacillus anthracis* CAP and PAG DNA Targets Based on the Incorporation of Tailed Primers and Ferrocene-Labeled dATP

Ivan Magriñá,[†] Miriam Jauset-Rubio,[†] Mayreli Ortiz,[†] Herbert Tomaso,[‡] Anna Simonova,[§,∥] Michal Hocek,*[,§,∥] and Ciara K. O'Sullivan*[,†,⊥]

[†]INTERFIBIO Consolidated Research Group, Departament d'Enginyeria Química, Universitat Rovira i Virgili, Avinguda Països Catalans 26, 43007 Tarragona, Spain

[‡]Friedrich-Loeffler-Institut, Naumburger Str. 96a, 07743 Jena, Germany

[§]Institute of Organic Chemistry and Biochemistry, Czech Academy of Sciences, Flemingovo nám. 2, CZ-16610 Prague, Czech Republic

[∥]Department of Organic Chemistry, Faculty of Science, Charles University in Prague, Hlavova 8, CZ-12843 Prague 2, Czech Republic

[⊥]Institució Catalana de Recerca i Estudis Avançats, Passeig Lluís Companys, 23, 08010 Barcelona, Spain

Supporting Information

ABSTRACT: We report the duplex amplification of two plasmid DNA markers involved in the virulence of *Bacillus anthracis*, CAP and PAG, and the direct electrochemical detection of these amplicons. The method consists of the simultaneous amplification of the two targets in a single-pot reaction via polymerase chain reaction (PCR) using tailed primers and ferrocene-labeled dATP. Following amplification, the PCR products hybridize to probes immobilized on electrodes in a microfabricated electrode array chip. The incorporated ferrocene labeled dATP is then detected using square wave voltammetry. We evaluated the effect of electrolyte cations, anions, and concentration to condense, bend, and shrink double-stranded DNA and their effect on the intensity of the ferrocene signal. We obtained detection limits of 0.8 and 3.4 fM for CAP and PAG targets, respectively. We successfully developed a method to detect the presence of both targets in genomic DNA extracted from real samples.

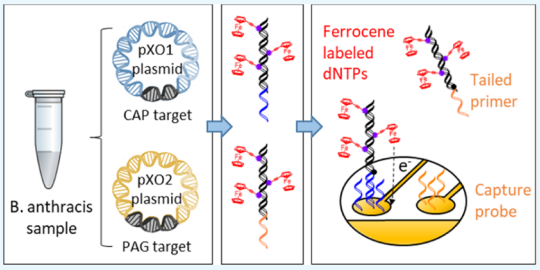

1. INTRODUCTION

Bacillus anthracis is a nonmotile, Gram-positive, rod-shaped, and spore-forming bacteria, known for being the causative agent of Anthrax.[1] It is an enzootic disease in most countries in Africa and Asia, but it also occurs sporadically in Europe, America, and Australia. Anthrax affects mainly herbivores but all mammals, including humans susceptible to infection. The infection starts when spores of *B. anthracis* enter the host body through skin injuries, an insect bite, by consuming contaminated food, and/or by inhalation of airborne spores. Generally, gastrointestinal and pulmonary infections are more severe, but even cutaneous infection, the most common form of infection in humans, can lead to fatal systemic anthrax.[2] The World Health Organization has published an extensive review on anthrax covering different aspects of the disease, including the disease and its importance, the etiology and ecology, the incidence, the transmission, the clinical manifestations, the treatment and prophylaxis in humans and animals, and directions for Anthrax control and surveillance.[1]

There are several reports describing methods for the detection of *B. anthracis*,[3] and those based on the detection of nucleic acids are very interesting because of the higher sensitivity and specificity that can be achieved as compared to antigen−antibody/aptamer-based detection systems. Most of the reports focus on the detection of two virulence plasmids, pXO1 and pXO2, which have been used to distinguish them from other bacteria in the *Bacillus cereus* group, such as *B. anthracis*, *B. cereus*, *Bacillus thuringiensis*, *Bacillus mycoides*, *Bacillus Psuedomycoides*, and *Bacillus wihenstephanensis*.[3] The pXO1 plasmid contains the genes for the toxin proteins: protective antigen [pagA], edema factor [cya], and lethal factor [lef], which work in tandem to produce edema and cell death. On the other hand, the pXO2 bears the genes capA, capB, and capC required for the capsule synthesis that facilitates evasion of the immune system. The number of pXO1 and pXO2 plasmid copies differs from strain to strain and are between 2 and 41 copies of pXO1 plasmid and 1−2 copies of pXO2 plasmid.[4]

Received: September 5, 2019
Accepted: November 21, 2019
Published: December 11, 2019

DOI: 10.1021/acsomega.9b02890
ACS Omega 2019, 4, 21900−21908

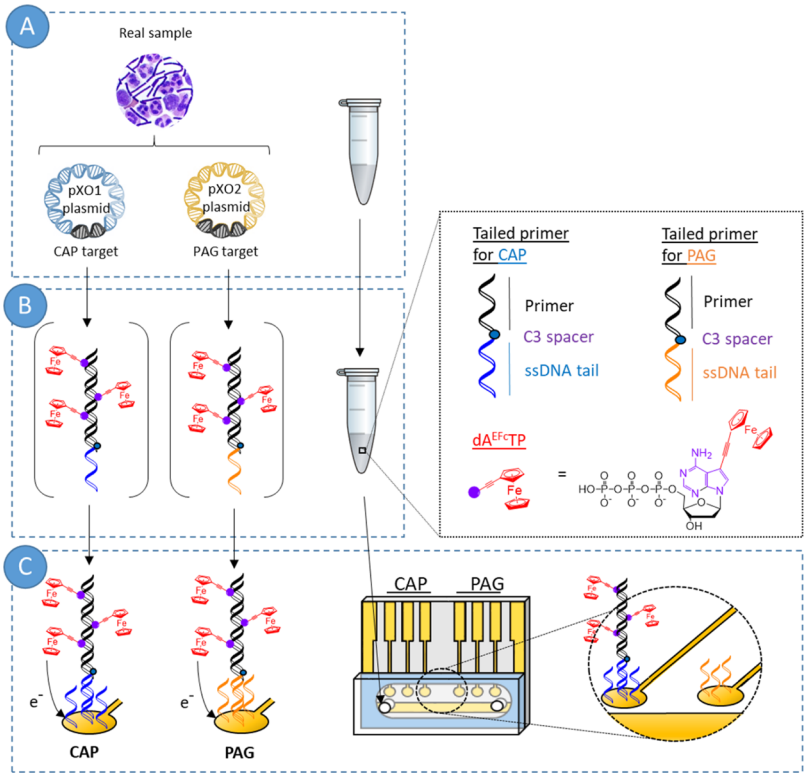

Figure 1. Schematic of the assay (A) Genomic DNA extraction from real samples including pXO1 and pXO2 plasmids, in case they are present. (B) Duplex DNA amplification in the presence of **dA^{EFc}TP** and tailed primers for CAP and PAG targets. (C) PCR product hybridization on a microarray electrode modified with a capture probe specific for each one of the targets, wash, and electrochemical detection.

The loss of any of the plasmids, which is common for pXO2 plasmid in nature but rare for the toxin plasmid pXO1, results in a strong strain attenuation.[2] In fact, vaccines for *B. anthracis* are made of strains that do not contain pXO1 plasmid (Pasteur vaccine) or strains that do not contain pXO2 plasmid (Sterne vaccine) because the absence of one of them highly decreases its virulence. Consequently, when developing a method to identify *B. anthracis* and assess its risks and potential effect on health, it is important not only to identify the species but also to determine if it contains both virulent plasmids.

Determination of pXO1 and pXO2 plasmids is reported for quantitative polymerase chain reaction (qPCR) setups because of its high sensitivity and the self-contained nature of the assay. Nevertheless, qPCR requires expensive and bulky instrumentation that hinders its applicability as a point-of-need method. As an alternative, electrochemical genosensors are emerging as an alternative approach to qPCR with advantages that include portability, low cost, and good analytical performance.[5]

Electrochemical genosensors combine the high sensitivity and robustness of electrochemistry-based sensors[6] with the selectivity provided by the specific DNA hybridization that occurs between complementary DNA strands. In most cases, genosensors require an initial enrichment of the target sequence to increase the target concentration to detectable levels, a step that is usually performed using polymerase chain reaction (PCR).[7] Following amplification, the majority of electrochemical genosensors require the generation of single-stranded DNA (ssDNA) from the PCR product for detection via hybridization to a specifically designed and immobilized capture oligonucleotide probe. Generation of ssDNA can be achieved using asymmetric PCR, where different ratios of primers are exploited,[7] or alternatively, via thermal denaturation and rapid cooling.[7] An attractive alternative is the selective enzymatic digestion of one of the DNA strands using, for example, T7 or lambda exonuclease and a phosphorothioate labeled forward primer, while another approach uses biotinylated primer, following the capture of the amplicon on streptavidin magnetic beads and thermal/pH denaturation to release ssDNA.[8] A different strategy reported recently takes advantage of the use of tailed primers, which consist of primers modified at the 5′- end with a single-stranded DNA sequence ("tail") that is used for hybridization. The tail is separated from the primer using a 3-C alkyl chain spacer to prevent the elongation of the tail during amplification.[9−13]

The detection of DNA following hybridization to the immobilized oligonucleotide probe can be achieved directly by direct oxidation of guanines,[14] but the majority of the reports to date describe the use of labels (organic dyes, metal complexes, enzymes, or metal particles) that bind to the target through a secondary labeled reporting probe or, alternatively, intercalate within the dsDNA, or are electrostatically adsorbed on the dsDNA backbone.[15]

The use of dNTPs modified with redox active labels presents a very interesting approach to directly produce a labeled amplicon and avoid the necessity of introducing a secondary labeled probe. Several redox labeled dNTPs have been reported including ferrocene,[16] anthraquinone,[17] benzofurazane,[18] and polyoxometalates.[19] Ferrocene is particularly of interest because it is a reversible and stable label with redox peaks within the potential window of a gold electrode, and furthermore, Fc-labeled dNTPs are efficiently incorporated by several DNA polymerases such as Klenow (exo-), DyNAzyme,[16] and Vent (exo-).[20] We have chosen 7-ferrocenylethynyl-7-deaza-dATP (**dA^{EFc}TP**) because it was previously

DOI: 10.1021/acsomega.9b02890
ACS Omega 2019, 4, 21900−21908

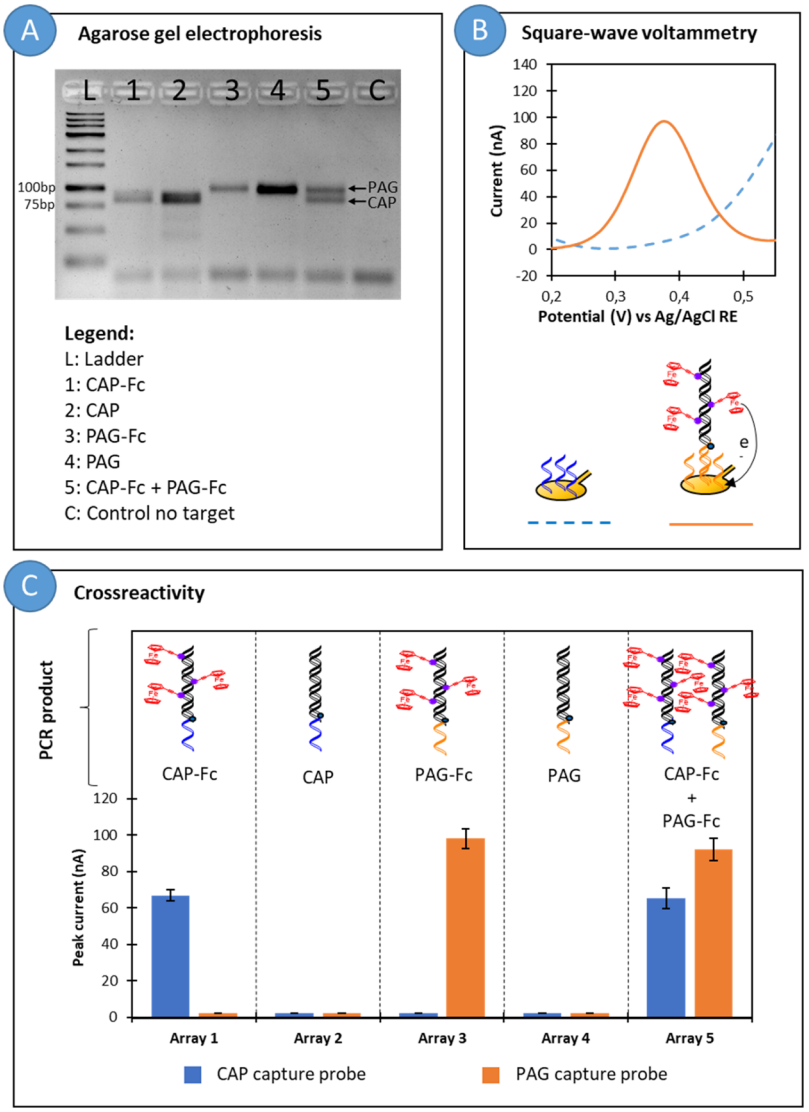

Figure 2. Hybridization and detection of amplified PCR products on the electrode array. (A) Agarose gel electrophoresis obtained after PCR amplification. (B) Voltammogram obtained for hybridization of PCR product #3 on the electrode array. (C) Peak intensites obtained for the other PCR products.

shown that 7-alkynyl-7-deazaadeninen are particularly good substrates for polymerases, even better than natural dATP.[21]

We recently reported a singleplex genosensor to determine the presence of *Karlodinium armiger* in seawater samples as a proof-of-concept of a novel approach, where we combined the use of tailed primers and **dA^{EFc}TP**.[22] This feasibility study highlighted the possibility of using this approach for detection of a single DNA sequence. In the work reported here, we wished to further show the immense possibilities of the approach by moving forward to a more challenging target that requires duplex parallel detection of two sequences. Duplex detection with two sets of tailed primers requires optimization to facilitate a single-pot amplification with duplex-target detection as opposed to two individual PCR reactions being detected on a single microarray. Probes designed to hybridize to the tails of each of the targets were immobilized on individual electrodes of a microarray and were evaluated for their specificity. Furthermore, we studied the effect of the electrolyte solution on the ferrocene oxidation peak because of shrinking, bending, and shielding effects, evaluating the effect of monovalent (K^+ and Na^+) and divalent (Mg^{2+}, Sr^{2+}, and Ca^{2+}) cations and the effect of a range of anions and the effect of the electrolyte concentration and pH. Using conditions optimized to provide maximum specificity and sensitivity, the genosensor array was exploited for the detection of the *B. anthracis* virulence factors CAP and PAG genes in real samples, and the flow-through assay is schematically depicted in Figure 1.

2. RESULTS AND DISCUSSION

2.1. PCR Product Hybridization and Cross Reactivity.

To demonstrate the method presented in this paper, we carried out five different PCR reactions to produce: #1. CAP-Fc, #2. CAP, #3. PAG-Fc, #4. PAG, and #5. CAP-Fc + PAG-Fc, where CAP or PAG refers to amplicon containing the CAP or PAG target sequence, respectively, and Fc indicates the presence of **dA^{EFc}TP** in the PCR mixture.

As we previously reported, the ratio **dA^{EFc}TP**/dATP affects the PCR amplification yield and the electrochemical signal obtained.[22] For most of the applications where the target concentration is in the range of fM, the ratio should be below

DOI: 10.1021/acsomega.9b02890
ACS Omega 2019, 4, 21900−21908

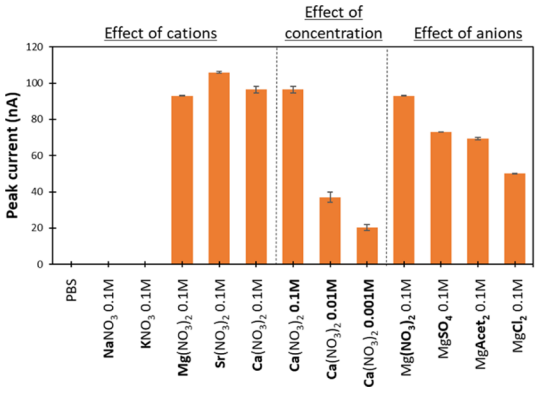

Electrolyte	pH	Peak current (nA) dsDNA	dsDNA-Fc
PBS	7.4	0	0
$NaNO_3$ 0.1M	6.5	0	0
KNO_3 0.1M	6.5	0	0
$Mg(NO_3)_2$ 0.1M	6.8	0	93.0 ± 0.2
$Sr(NO_3)_2$ 0.1M	6.4	0	105.9 ± 0.4
$Ca(NO_3)_2$ 0.1M	6.6	0	96.4 ± 1.9
$Ca(NO_3)_2$ 0.01M	6.6	0	36.9 ± 2.8
$Ca(NO_3)_2$ 0.001M	6.5	0	20.4 ± 1.7
$MgSO_4$ 0.1M	7.2	0	73.0 ± 0.1
$MgAcet_2$ 0.1M	6.5	0	69.3 ± 0.7
$MgCl_2$ 0.1M	6.6	0	50.0 ± 0.2

Figure 3. Effect of cations, anions, and electrolyte concentration on intensity of the ferrocene signal.

40% to amplify the target to detectable levels. We performed all the experiments with 20% **dA^{EFc}TP**/dATP ratio as it allowed us to amplify both targets at the same time and obtain good electrochemical signals.

As can be seen in Figure 2a, gel electrophoresis analysis revealed that the duplex PCR product with the **dA^{EFc}TP** incorporated produces two distinguishable bands, with band intensities similar to the singleplex amplification of each of CAP and PAG with **dA^{EFc}TP**. The difference in band intensities between both the CAP and PAG, with and without the **dA^{EFc}TP,** is probably caused by the presence of bulky ferrocene moiety in the template which can lower the PCR yield because of the difficult reading of the polymerase through the hypermodified DNA strand.[23]

Subsequently, we added each of the PCR products (#1−5) to a different electrode array and then allowed them to incubate for 30 min at room temperature (22 °C), washed the arrays with PBS Tween, and detected the presence of ferrocene using square wave voltammetry in the presence of 100 mM $Ca(NO_3)_2$. Figure 2b shows an example of the voltammograms obtained for array number 3. The voltammograms obtained for the other electrode arrays can be seen in Supporting Information (Figure S1). Only the electrodes modified with the capture probe for the PAG target showed a ferrocene oxidation peak at 360 mV when incubated with the PCR product #3. There was no ferrocene oxidation peak observed for the electrodes modified with the capture probe for the CAP target, indicating that there is no nonspecific adsorption on the electrodes or cross-reactivity between the tails. Figure 2c shows the ferrocene peak currents obtained for the rest of the PCR products when incubated, washed, and measured with the electrode array. As expected, only the PCR products containing ferrocene give an oxidation peak, and the peak is only observed for the electrodes modified with the specific capture probe. We observed that the ferrocene peak obtained for PAG is higher than the ferrocene peak obtained for CAP, even if the starting DNA concentration for both targets in the PCR mixture is the same. We attribute this difference to the different content of adenosine in the target sequences (PAG has 45 and CAP 36). Brázdilova et al.[16] previously reported the peak intensity dependence on the number of **dA^{EFc}TP** incorporated in the DNA. Additionally, we also observed no significant differences between the singleplex product and the duplex product for each of the targets, which suggests that neither of the targets supress or inhibit the amplification of the other target.

2.2. Effect of Electrolyte on the Ferrocene Oxidation Peak. We studied the effect of the electrolyte solution on the ferrocene oxidation peak. We assessed the effect of the cation, the effect of the anion, and the effect of the electrolyte concentration in the pH range between 6 and 7.4 and at a constant temperature of 25 °C (Figure 3). We could not observe the ferrocene oxidation peak in the presence of PBS and other electrolytes containing monovalent cations such as K^+ and Na^+. We hypothesize that the ferrocenes could not reach the electrode surface to allow the electron transfer because of the two main factors: (a) the poor mobility of the ferrocene confined in the double-stranded DNA (dsDNA) structure and (b) the repulsion experienced by captured PCR amplicons hybridized to the electrode-tethered probes, with neighboring PCR amplicons and the ssDNA capture probes immobilized on the electrode surface.

However, we clearly observed the ferrocene oxidation peak in the presence of the divalent cations: Ca^{2+}, Mg^{2+}, and Sr^{2+}. We postulate that this is due to the ability of divalent cations to: (a) condense and shrink dsDNA,[24] (b) bend dsDNA,[25] and (c) shield the electrostatic repulsions between neighboring DNA strands,[26] with the combination of these effects contributing to bringing the ferrocenes closer to the electrode surface, facilitating electron transfer.

We also observed a decrease in the ferrocene peak intensity when we decreased the concentration of the electrolyte $Ca(NO_3)_2$ from 0.1 to 0.001 M, which we attribute to less cation molecules being available at lower electrolyte concentrations, and less notable shrinking, bending, and shielding effect thus occurs.

Finally, we observed that the ferrocene peak intensity also depends on the nature of the anion present in the solution we tested: NO_3^-, acetate$^-$, SO_4^{2-}, and Cl^-. This phenomenon is more difficult to explain because anions are rarely considered in the first hydration shell of the DNA because of the negatively charged nature of the DNA phosphate backbone which repels anions and attracts cations. However, there are studies that demonstrate that DNA has electropositive edges which involve amino, imino, and hydroxyl groups that can act as binding points for anions.[27]

We chose $Ca(NO_3)_2$ 0.1 M as the preferred electrolyte solution to perform further experiments, but $Mg(NO_3)_2$ 0.1 M or $Sr(NO_3)_2$ 0.1 M could also be used, and the same results are obtained.

2.3. Duplex Calibration Curve and Real Samples. We performed a PCR duplex calibration curve covering a wide range of starting DNA concentrations, from 100 aM to 10 pM

DOI: 10.1021/acsomega.9b02890
ACS Omega 2019, 4, 21900−21908

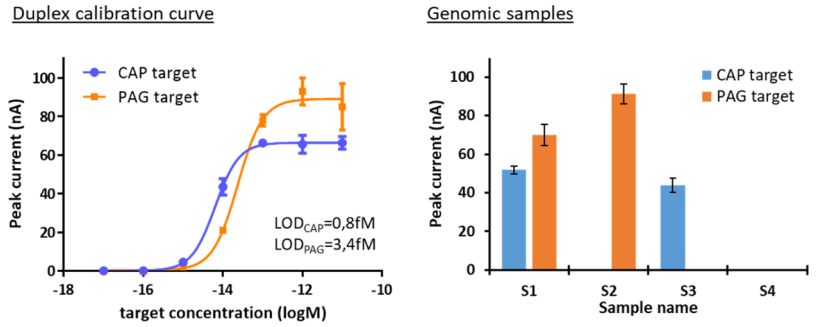

Figure 4. Duplex calibration curve performed with synthetic DNA and genomic samples.

using a 20% **dA^{EFc}TP**/dATP ratio. We observed that the ferrocene signal is saturated for both CAP and PAG targets at concentrations between 100 fM and 10 pM, and that no signal is observed for concentrations equal to or below 100 aM. We used GraphPad Prism software to plot the peak current versus initial target concentration and applied a sigmoidal curve fit. The limit of detection (LOD) was calculated as the blank value plus three times the standard deviation of the blank value. We obtained detection limits of 0.8 and 3.4 fM for CAP and PAG targets, respectively (Figure 4). A higher number of PCR cycles could be used to decrease the LOD, but this also results in nonspecific amplicons bearing the tail, that will be detected as false positives.

The same PCR conditions were used to determine the presence of CAP and PAG targets in 4 genomic DNA extracts from real samples: S1, S2, S3, and S4. We only observed ferrocene peaks for CAP and/or PAG for the samples, where we expected to find the targets, according to the data provided by FLI and the qPCR experiment carried out in house (Table 1).

Table 1. Samples and Presence of Plasmids

	provided by collaborator		estimated by qPCR		estimated by this method	
genomic samples	pOX1 plasmid	pOX2 plasmid	PAG presence	CAP presence	PAG presence	CAP presence
S1	+	+	+	+	+	+
S2	+	−	+	−	+	−
S3	−	+	−	+	−	+
S4	−	−	−	−	−	−

In order to identify the presence of *B. anthracis* and its virulence, we chose to detect the pag and cap genes present in the virulence plasmids pXO1 and pXO2, respectively. The bases are similar to commercial kits that are based on the target amplification of virulence plasmid markers cya, lef of pag for pXO1, and cap for pXO2, where the main differences rely on the detection strategy of the amplification product. While we used ferrocene-labeled dATP to generate redox active amplicons that we detected following hybridization to specifically designed probes immobilized on individual gold electrodes of an array, the commercial kits are based on detection of the amplicon using fluorescent probes. Examples of commercially available kits include: Applied Biosystems TaqMan *B. anthracis* Detection Kit, based on a dual singleplex assay for pXO1 and pXO2, AmpliSens *B. anthracis*-FRT based on the triplex detection of pagA, capA genes, and an internal control, and RealArt *B. anthracis* PCR from Arthus Biotech, based on the detection of lef and capA targets.

Apart from the commercially available kits there are many reports describing nucleic-based methods to detect *B. anthracis*.[3] The majority of these are based on the detection of the mentioned virulent plasmid markers, but there are other nonplasmid targets described in the literature, including the chromosomal markers BA-5449,[28] BA-5510,[29] gyrA,[30] rpoB[31] pIcR,[32] and AC-390[33] and variable number tandem repeats present in an open reading frame.[34] While these markers are useful for the identification of *B. anthracis*, they cannot be used to predict the virulence of the strain, as this is dependent on the presence of the virulence plasmids pXO1 and pXO2.

An electrochemical genosensor to detect the specific *B. anthracis* regulatory gene atxA was recently reported,[35] based on the post-asymmetric amplification and hybridization of the target, with differential pulse voltammetric detection of the redox intercalator methylene blue. The LOD is higher than the one presented in this paper (1 pM vs 1 fM), and the amplification time is longer (132 vs 90 min), and while the method was useful for the identification of *B. anthracis*, it did not determine the presence of pXO1 and pXO2 and thus could not predict its virulence.

Another recent approach consisted of the isothermal real time recombinase polymerase amplification of four different markers, the BA-5345 chromosomal marker, lef factor (pXO1), capA (pxO2), and adk marker from the *B. cereus* group. The method has been used and validated in field achieving an LOD of 10 copies in less than 10 min but requires four singleplex reactions, instead of a single one-pot multiplex reaction.[36]

Our approach is significantly more facile than many of these reported approaches, being able to simultaneously but individually and quantitatively detect each of the pXO1 and pXO2, at low femtomolar detection limits using duplex amplification and detection. The use of the tailed primers overcomes the need for the generation of ssDNA, which is not only laborious and costly but also significant, and uncontrollable amounts of DNA are often lost while producing the ssDNA. The use of the Fc-dATP facilitates direct electrochemical detection of the tailed amplicon product, significantly simplifying the assay, and we are currently working on the use of isothermal amplification to further move this approach toward an effective platform, which can be deployed and used at the point-of-need/care.

3. CONCLUSIONS

We presented a novel duplex electrochemical genosensor for the simultaneous amplification and detection of 2 DNA sequences, that is, two plasmid DNA markers involved in the virulence of *B. anthracis*, CAP and PAG, in genomic DNA extracted from real samples. The main advantages of the

DOI: 10.1021/acsomega.9b02890
ACS Omega 2019, 4, 21900−21908

method include the amplification of both targets in a single-pot reaction and the direct hybridization and detection of the PCR product on an electrode microarray. The method overcomes some of the limitations of classic genosensors, including the need to generate ssDNA for hybridization purposes, thanks to the use of tailed primers and the need for posthybridization labeling methods because of the use of ferrocene-labeled dATP, the combination of both decreasing the number of steps required. We also studied the effect of electrolyte cations, anions, and concentration on the ferrocene signal and postulated that the enhancement in the signal observed in the presence of divalent cations is because of their ability to condense, bend, and shrink double-stranded DNA, while shielding the electrostatic repulsions between neighboring DNA strands and culminating in the ferrocenes being closer to the electrode surface, thus enhancing electron transfer. The method presented here is completely generic in nature and transferable to other targets for duplex or multiplex simultaneous detection of several DNA targets. In order to implement the use of tailed primers and **dA^{EFc}TP** for use at the point-of-need, we are currently exploring multiplex isothermal amplification combined with electrochemical detection using a handheld potentiostat.

4. EXPERIMENTAL SECTION

4.1. Reagents and Materials. For PCR experiments, we used KOD XL polymerase purchased from Merck Millipore (Madrid, Spain), synthetic oligonucleotides obtained from Biomers (Ulm, Germany), natural dNTPs from ThermoFischer Scientific (Barcelona, Spain), and **dA^{EFc}TP** synthesized following the Sonogashira reaction.[16] For qPCR experiments, we used the PowerUp SYBRGreen master mix from Applied Biosystems.

For agarose gel electrophoresis, we employed certified molecular biology agarose gel powder from ThemoFischer Scientific (Barcelona, Spain), GelRed Nucleic Acid Gel Stain from Biotium (Barcelona, Spain), Tris-borate-EDTA (TBE) buffer prepared in house (10.8 g of TRIS-base, 5.5 g of boric acid, and 4 mL of ETDA 0.5 M per liter of solution), and the DNA gene ruler low range DNA Ladder from Thermo Scientific.

To fabricate the electrode array and microfluidics, we used soda-lime glass slides from Sigma-Aldrich (Spain), three-millimeter thick polymethylmethacrylate (PMMA) from La Indústria de la Goma (Tarragona, Spain), and double-sided adhesive gasket ARSeal 90880 from Adhesive Research (Ireland).

All other chemicals were obtained from Sigma-Aldrich S.A. (Barcelona, Spain) and used as received.

We used DNA free water provided by Fisher Bioreagents to prepare PCR solutions and high purity deionized water (18 MΩ) produced with a Milli-Q RG system (Millipore Ibérica, Spain) for all other solutions.

4.2. Oligonucleotide Sequences. We modified the previously published primers for the detection of CAP and PAG genes[37,38] by the addition of two different tails on the forward primers: CAP FwP and PAG FwP. The specificity of these primers was checked using Primer Blast software. In addition, the multiple primer analyzer from ThermoFischer Scientific was used to test the cross-reactivity between the different primers designed, so that the designed primers avoid the formation of self-dimers and primer-dimers. Table 2 details the oligonucleotides and modifications used in this work.

Table 2. List of Oligonucleotides[a]

oligo name	Sequence
CAP FwP	5′-*ATT ACG ACG AAC TCA ATG AA*-C3-TTG GGA ACG TGT GGA TGA TTT-3′
CAP RvP	5′-TCA GGG CGG CAA TTC ATA AT-3′
CAP CP	5′-*TTC ATT GAG TTC GTC GTA AT*T TTT TTT TTT TTT TT-3′-C6-THIOL
CAP target	5′-TTG GGA ACG TGT GGA TGA TTT TGG ATA TAG TAA TCT AGC TCC AAT TGT AAT TAT GAA TTG CCG CCC TGA-3′
PAG FwP	5′-*CTA AGT AGC CGA ATT CCT AG*-C3-CGG ATA GCG GCG GTT AAT C-3′
PAG RvP	5′-CAA ATG CTA TTT TAA GGG CTT CTT TT-3′
PAG CP	5′-*CTA GGA ATT CGG CTA CTT AG*T TTT TTT TTT TTT TT-3′-C6-THIOL
PAG target	5′-CGG ATA GCG GCG GTT AAT CCT AGT GAT CCA TTA GAA ACG ACT AAA CCG GAT ATG ACA TTA AAA GAA GCC CTT AAA ATA GCA TTT G-3′

[a]In bold: oligo modifications. In italics and underlined: sequences used for DNA hybridization: tails and surface probe.

4.3. Real Samples. The Friedrich-Loeffler-Institut (FLI) kindly provided us with purified genomic DNA samples, positive for *B. anthracis*, following the protocol described in the QIAamp DNA Mini Kit from Qiagen. Table 1 shows the presence of the plasmid pXO1, and/or the plasmid pXO2 for each of the samples according to the FLI Institute, to the qPCR experiments, and to the method presented here.

4.4. Polymerase Chain Reaction. We performed PCR in a T100 thermal cycler (Biorad) following the next step cycling protocol: 95 °C for 2 min, followed by 34 cycles at 95 °C for 30 s, 60 °C for 30 s, and 72 °C for 45 s, with a final elongation step at 72 °C for 5 min. Each 10 μL reaction mixture had 0.1 units of KOD XL, KOD XL buffer 1X, CAP primers (CAP FwP and CAP RvP) at 100 nM each one, PAG primers (PAG FwP and PAG RvP) at 100 nM each one, dGTP, dCTP, dTTP at 200 μM, and dATP at 160 μM and **dA^{EFc}TP** at 40 μM and finally 1 μL of the sample (Table 3).

Table 3. Reagents Used in the PCR Mixture

	sample name				
Reagents	CAP-Fc	CAP	PAG-Fc	PAG	CAP-Fc + PAG-Fc
dA^{EFc}TP/dATP ratio 20%	+	−	+	−	+
CAP target 100 fM	+	+	−	−	+
PAG target 100 fM	−	−	+	+	+

4.5. Agarose Gel Electrophoresis. We visualized the PCR products using agarose gel electrophoresis. The gel was prepared with ultralow pure agarose (4% w/v) in 1× TBE buffer and stained with GelRednucleic acid stain. We loaded 3 μL of the PCR product with 3 μL of loading buffer 2× per well, performed electrophoresis at 100 V for 1 h, and imaged the gels in a UV transilluminator at λ = 254 nm.

4.6. Quantitative Polymerase Chain Reaction. We performed qPCR assay using a real time thermocycler 7900HT from Applied Biosystems and a two-step cycling protocol with an initial denaturation step at 95 °C for 10 min, followed by 40 cycles at 95 °C for 20 s and 60 °C for 30 s. The reaction mixture contained SYBR Green dye 1×, CAP primers (CAP FwP and CAP RvP) at 100 nM each one, 100 nM of each of

DOI: 10.1021/acsomega.9b02890
ACS Omega 2019, 4, 21900−21908

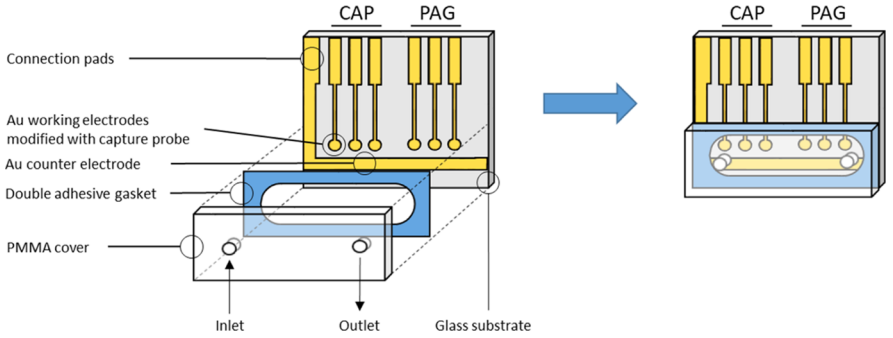

Figure 5. Scheme of the electrode array and the microfluidic cell.

the PAG primers (PAG FwP and PAG RvP), and different concentrations of the target DNA or the sample diluted in the qPCR mixture 10 times. The amplification plots for CAP and PAG targets and genomic DNA samples are included in the Supporting Information (Figures S1 and S2).

4.7. Electrode Fabrication. We designed an electrode array with a set of six circular gold working electrodes (1 mm^2) and a rectangular gold counter electrode (8 mm^2), Figure 5. To fabricate the array, we used soda-lime glass slides as the substrate, and we deposited the 30 nm Ti layer and the 100 nm Au layer by sputtering, as described previously.[39] Briefly, we deposited a positive photoresist AZ1505 (MicroChemicals GmbH, Germany) via spin coating at 4000 rpm for 30 s on a precleaned and dried glass slide. We then placed and aligned a chromium mask in the contact mode on the photoresist coated glass slide, which was subsequently exposed to UV light for 4 s (LED Paffrath GmbH, Rose FotoMasken, Germany), and the photoresist was developed using the commercial developer AZ726. We then introduced the glass slide into the sputtering chamber (ATC Orion 8-HV, AJA Interna-tional Inc., USA) for oxygen plasma etching using AC O_2/Ar (5 $cm^3 \cdot s^{-1}$ of Ar, 5 $cm^3 \cdot s^{-1}$ of O_2, 50 W) for 5 min, using a sputtering deposition of the 30 nm Ti/TiO_2 layer (oxygen flow rate: 5 $cm^3 \cdot s^{-1}$ of O_2 for the first 10 nm, which was then increased to 20 $cm^3 \cdot s^{-1}$ for the last 20 nm. Ar flow rate: constant 5 $cm^3 \cdot s^{-1}$) and a sputtering deposition on the 100 nm Au layer by AC sputtering (5 $cm^3 \cdot s^{-1}$ of Ar, 5 $cm^3 \cdot s^{-1}$ of O_2, 50 W). Finally, we performed the lift-off step by sonication in acetone for 5 min, then sonication in isopropanol for 5 min, and finally, we rinsed the glass slide with Milli-Q water and dried with N_2.

4.8. Electrode Functionalization with Capture Probe. Prior to functionalization, we washed the electrode arrays with soap, then rinsed them with Milli-Q water, and finally dried them with N_2. We then dropcasted 1 μL of a surface probe cocktail on each working electrode, and the array was then incubated overnight (at least 16 h) at room temperature (22 °C) in a humidity saturated chamber. The probe cocktail contained 1 μM capture probe (CAP capture or PAG capture), 100 μM mercaptohexanol, and 1 M KH_2PO_4. After functionalization, we rinsed the electrodes with abundant Milli-Q and dried them with N_2.

4.9. Microfluidic Fabrication and Mounting. We designed microfluidic chambers of 15 μL volume to host the PCR product for amplicon hybridization and electrochemical detection (Figure 5). The chamber is achieved by adhering the electrode array to a PMMA cover using a double adhesive gasket. We used Winrad software to design the patterns and a CO_2 laser marker (Fenix, Synrad, USA) to cut the materials. Once assembled, we washed the microfluidic chambers with 200 μL of PBS Tween-20, then 200 μL of Milli-Q and finally dried them with N_2 prior to use.

4.10. Amplicon Hybridization on Electrode Arrays. After PCR, we injected 15 μL of the PCR product into the microfluidic chamber housing the electrode array. Hybridization took place at room temperature (22 °C) in a humidity saturated chamber for 30 min. We then flushed the microfluidic chamber 3 times, with 200 μL of PBS Tween-20 and then with 200 μL of $Mg(NO_3)_2$ 0.1 M.

4.11. Electrochemical Measurements. We performed square wave voltammetry using a potentiostat/galvanostat PBSTAT 12 Autolab controlled with Nova 2.1.3 software. We took the measurements following hybridization in a $Mg(NO_3)_2$ 0.1 M electrolyte solution using an external Ag/AgCl reference electrode and the internal counter and working gold electrodes on the electrode array. We stepped the potential from 0 to 0.6 V with a 5 mV step, 25 mV modulation amplitude and 50 Hz of frequency. The potentiostat and electrode array were connected using an "in-house" connector.

■ ASSOCIATED CONTENT

Supporting Information

The Supporting Information is available free of charge at https://pubs.acs.org/doi/10.1021/acsomega.9b02890.

Square wave voltammograms and qPCR amplification plots (PDF)

■ AUTHOR INFORMATION

Corresponding Authors

*E-mail: michal.hocek@uochb.cas.cz (M.H.).
*E-mail: ciara.osullivan@urv.cat (C.K.O.).

ORCID

Michal Hocek: 0000-0002-1113-2047
Ciara K. O'Sullivan: 0000-0003-2603-2230

Notes

The authors declare no competing financial interest.

■ ACKNOWLEDGMENTS

The authors gratefully acknowledge the financial support from Spanish Ministerio de Economía y Competitividad for CIGUASENSING BIO2017-87946-C2-1-R and SEASENSING BIO2014-56024-C2-1. The work was also supported by the Czech Academy of Sciences (Praemium Academiae to M.H.), and by the European Regional Development Fund; OP RDE (no. CZ.02.1.01/0.0/0.0/16_019/0000729 to M.H.).

DOI: 10.1021/acsomega.9b02890
ACS Omega 2019, 4, 21900−21908

REFERENCES

(1) WHO. *Anthrax in Humans and Animals*; World Organisation for Animal Health, 2008; p 219.

(2) Mock, M.; Fouet, A. Anthrax. *Annu. Rev. Microbiol.* **2001**, *55*, 647−671.

(3) Rao, S. S.; Mohan, K. V. K.; Atreya, C. D. Detection Technologies for Bacillus Anthracis: Prospects and Challenges. *J. Microbiol. Methods* **2010**, *82*, 1−10.

(4) Straub, T.; Baird, C.; Bartholomew, R. A.; Colburn, H.; Seiner, D.; Victry, K.; Zhang, L.; Bruckner-Lea, C. J. Estimated Copy Number of Bacillus Anthracis Plasmids PXO1 and PXO2 Using Digital PCR. *J. Microbiol. Methods* **2013**, *92*, 9−10.

(5) Manzanares-palenzuela, C. L.; Martín-Fernández, B.; Sánchez-Paniagua López, M.; López-Ruiz, B. Trends in Analytical Chemistry Electrochemical Genosensors as Innovative Tools for Detection of Genetically Modified Organisms. *Trends Anal. Chem.* **2015**, *66*, 19−31.

(6) Wang, J. Towards Genoelectronics: Electrochemical Biosensing of DNA Hybridization. *Chem.—Eur. J.* **1999**, *5*, 1681−1685.

(7) Tosar, J. P.; Brañas, G.; Laíz, J. Electrochemical DNA Hybridization Sensors Applied to Real and Complex Biological Samples. *Biosens. Bioelectron.* **2010**, *26*, 1205−1217.

(8) Svobodová, M.; Pinto, A.; Nadal, P.; O'Sullivan, C. K. Comparison of Different Methods for Generation of Single-Stranded DNA for SELEX Processes. *Anal. Bioanal. Chem.* **2012**, *404*, 835−842.

(9) Jauset-Rubio, M.; Svobodová, M.; Mairal, T.; McNeil, C.; Keegan, N.; El-Shahawi, M. S.; Bashammakh, A. S.; Alyoubi, A. O.; O'Sullivan, C. K. Aptamer Lateral Flow Assays for Ultrasensitive Detection of β-Conglutin Combining Recombinase Polymerase Amplification and Tailed Primers. *Anal. Chem.* **2016**, *88*, 10701−10709.

(10) Jauset-Rubio, M.; Svobodová, M.; Mairal, T.; McNeil, C.; Keegan, N.; Saeed, A.; Abbas, M. N.; El-Shahawi, M. S.; Bashammakh, A. S.; Alyoubi, A. O.; et al. Ultrasensitive, Rapid and Inexpensive Detection of DNA Using Paper Based Lateral Flow Assay. *Sci. Rep.* **2016**, *6*, 37732.

(11) Jauset-Rubio, M.; Tomaso, H.; El-Shahawi, M. S.; Bashammakh, A. S.; Al-youbi, A. O.; O'Sullivan, C. K. Duplex Lateral Flow Assay for the Simultaneous Detection of Yersinia Pestis and Francisella Tularensis. *Anal. Chem.* **2018**, *90*, 12745−12751.

(12) Al-madhagi, S.; Joda, H.; Jauset-rubio, M.; Ortiz, M.; Katakis, I.; O'Sullivan, C. K. Isothermal Amplification Using Modi Fi Ed Primers for Rapid Electrochemical Analysis of Coeliac Disease Associated DQB1*02 HLA Allele. *Anal. Biochem.* **2018**, *556*, 16−22.

(13) Joda, H.; Beni, V.; Willems, A.; Frank, R.; Höth, J.; Lind, K.; Strömbom, L.; Katakis, I.; O'Sullivan, C. K. Modified Primers for Rapid and Direct Electrochemical Analysis of Coeliac Disease Associated HLA Alleles. *Biosens. Bioelectron.* **2015**, *73*, 64−70.

(14) Ferapontova, E. E. DNA Electrochemistry and Electrochemical Sensors for Nucleic Acids. *Annu. Rev. Anal. Chem.* **2018**, *11*, 197−218.

(15) Kerman, K.; Kobayashi, M.; Tamiya, E. Recent Trends in Electrochemical DNA Biosensor Technology. *Meas. Sci. Technol.* **2004**, *15*, R1−R11.

(16) Brázdilová, P.; Vrábel, M.; Pohl, R.; Pivoňková, H.; Havran, L.; Hocek, M.; Fojta, M. Ferrocenylethynyl Derivatives of Nucleoside Triphosphates: Synthesis, Incorporation, Electrochemistry, and Bioanalytical Applications. *Chem.—Eur. J.* **2007**, *13*, 9527−9533.

(17) Balintová, J.; Pohl, R.; Horáková, P.; Vidláková, P.; Havran, L.; Fojta, M.; Hocek, M. Anthraquinone as a Redox Label for DNA: Synthesis, Enzymatic Incorporation, and Electrochemistry of Anthraquinone-Modified Nucleosides, Nucleotides, and DNA. *Chem.—Eur. J.* **2011**, *17*, 14063−14073.

(18) Balintová, J.; Plucnara, M.; Vidláková, P.; Pohl, R.; Havran, L.; Fojta, M.; Hocek, M. Benzofurazane as a New Redox Label for Electrochemical Detection of DNA: Towards Multipotential Redox Coding of DNA Bases. *Chem.—Eur. J.* **2013**, *19*, 12720−12731.

(19) Ortiz, M.; Debela, A. M.; Svobodova, M.; Thorimbert, S.; Lesage, D.; Cole, R. B.; Hasenknopf, B.; O'Sullivan, C. K. PCR Incorporation of Polyoxometalate Modified Deoxynucleotide Triphosphates and Their Application in Molecular Electrochemical Sensing of Yersinia Pestis. *Chem.—Eur. J.* **2017**, *23*, 10597−10603.

(20) Wlassoff, W. A.; King, G. C. Ferrocene Conjugates of DUTP for Enzymatic Redox Labelling of DNA. *Nucleic Acids Res.* **2002**, *30*, No. e58.

(21) Kielkowski, P.; Fanfrlík, J.; Hocek, M. 7-Aryl-7-Deazaadenine 2′-Deoxyribonucleoside Triphosphates (DNTPs): Better Substrates for DNA Polymerases than DATP in Competitive Incorporations. *Angew. Chem., Int. Ed.* **2014**, *53*, 7552−7555.

(22) Magriñá, I.; Toldrà, A.; Campàs, M.; Ortiz, M.; Simonova, A.; Katakis, I.; Hocek, M.; O'Sullivan, C. K. Electrochemical Genosensor for the Direct Detection of Tailed PCR Amplicons Incorporating Ferrocene Labelled DATP. *Biosens. Bioelectron.* **2019**, *134*, 76−82.

(23) Zhu, Z.; Waggoner, A. S. Molecular Mechanism Controlling the Incorporation of Fluorescent Nucleotides into DNA by PCR. *Cytometry* **1997**, *28*, 206−211.

(24) Tongu, C.; Kenmotsu, T.; Yoshikawa, Y.; Zinchenko, A. A.; Chen, N.; Yoshikawa, K. Competitive Effects of 2 + and 3 + Cations on DNA Compaction. 1−15. **2016**.

(25) Rouzina, I.; Bloomfield, V. A. DNA Bending by Small, Mobile Multivalent Cations. *Biophys. J.* **1998**, *74*, 3152−3164.

(26) Špringer, T.; Sípová, H.; Vaisocherová, H.; Stepánek, J.; Homola, J. Shielding Effect of Monovalent and Divalent Cations on Solid-Phase DNA Hybridization: Surface Plasmon Resonance Biosensor Study. *Nucleic Acids Res.* **2010**, *38*, 7343−7351.

(27) Auffinger, P.; Bielecki, L.; Westhof, E. Anion Binding to Nucleic Acids. *Structure* **2004**, *12*, 379−388.

(28) Volokhov, D.; Pomerantsev, A.; Kivovich, V.; Rasooly, A.; Chizhikov, V. Identification of Bacillus Anthracis by Multiprobe Microarray Hybridization. *Diagn. Microbiol. Infect. Dis.* **2004**, *49*, 163−171.

(29) Olsen, J. S.; Skogan, G.; Fykse, E. M.; Rawlinson, E. L.; Tomaso, H.; Granum, P. E.; Blatny, J. M. Genetic Distribution of 295 Bacillus Cereus Group Members Based on Adk-Screening in Combination with MLST (Multilocus Sequence Typing) Used for Validating a Primer Targeting a Chromosomal Locus in B. Anthracis. *J. Microbiol. Methods* **2007**, *71*, 265−274.

(30) Hurtle, W.; Bode, E.; Kulesh, D. A.; Kaplan, R. S.; Garrison, J.; Bridge, D.; House, M.; Frye, M. S.; Loveless, B.; Norwood, D. Detection of the Bacillus Anthracis GyrA Gene by Using a Minor Groove Binder Probe. *J. Clin. Microbiol.* **2004**, *42*, 179−185.

(31) Almeida, J. L.; Harper, B.; Cole, K. D. Bacillus Anthracis Spore Suspensions: Determination of Stability and Comparison of Enumeration Techniques. *J. Appl. Microbiol.* **2008**, *104*, 1442−1448.

(32) Gierczyński, R.; Zasada, A. A.; Raddadi, N.; Merabishvili, M.; Daffonchio, D.; Rastawicki, W.; Jagielski, M. Specific Bacillus Anthracis Identification by a PlcR-Targeted Restriction Site Insertion-PCR (RSI-PCR) Assay. *FEMS Microbiol. Lett.* **2007**, *272*, 55−59.

(33) Cherif, A.; Borin, S.; Rizzi, A.; Ouzari, H.; Boudabous, A.; Daffonchio, D. Characterization of a Repetitive Element Polymorphism-Polymerase Chain Reaction Chromosomal Marker That Discriminates Bacillus Anthracis from Related Species. *J. Appl. Microbiol.* **2002**, *93*, 456−462.

(34) Jackson, P. J.; Walthers, E. A.; Kalif, A. S.; Richmond, K. L.; Adair, D. M.; Hill, K. K.; Kuske, C. R.; Andersen, G. L.; Wilson, K. H.; Hugh-Jones, M. E.; et al. Characterization of the Variable-Number Tandem Repeats in VrrA from Different Bacillus Anthracis Isolates. *Appl. Environ. Microbiol.* **1997**, *63*, 1400−1405.

(35) Das, R.; Goel, A. K.; Sharma, M. K.; Upadhyay, S. Electrochemical DNA Sensor for Anthrax Toxin Activator Gene AtxA-Detection of PCR Amplicons. *Biosens. Bioelectron.* **2015**, *74*, 939−946.

(36) Bentahir, M.; Ambroise, J.; Delcorps, C.; Pilo, P.; Gala, J.-L. Sensitive and Specific Recombinase Polymerase Amplification Assays for Fast Screening, Detection, and Identification of Bacillus Anthracis in a Field Setting. *Appl. Environ. Microbiol.* **2018**, *84*, No. e00506.

(37) Matero, P.; Hemmilä, H.; Tomaso, H.; Piiparinen, H.; Rantakokko-Jalava, K.; Nuotio, L.; Nikkari, S. Rapid Field Detection

DOI: 10.1021/acsomega.9b02890
ACS Omega 2019, 4, 21900−21908

Assays for Bacillus Anthracis, Brucella Spp., Francisella Tularensis and Yersinia Pestis. *Clin. Microbiol. Infect.* **2011**, *17*, 34−43.
(38) Skottman, T.; Piiparinen, H.; Hyytiäinen, H.; Myllys, V.; Skurnik, M.; Nikkari, S. Simultaneous Real-Time PCR Detection of Bacillus Anthracis , Francisella Tularensis and Yersinia Pestis. *Eur. J. Clin. Microbiol. Infect. Dis.* **2006**, *26*, 207−211.
(39) del Río, J. S.; Svobodova, M.; Bustos, P.; Conejeros, P.; O'Sullivan, C. K. Electrochemical Detection of Piscirickettsia Salmonis Genomic DNA from Salmon Samples Using Solid-Phase Recombinase Polymerase Amplification. *Anal. Bioanal. Chem.* **2016**, *408*, 8611−8620.

DOI: 10.1021/acsomega.9b02890
ACS Omega 2019, 4, 21900−21908